J. Environ. Nanotechnol.
Volume 3, No.3 pp. 121-128
ISSN (Print): 2279-0748
ISSN (Online): 2319-5541
doi: 10.13074/jent.2014.09.143116

Synthesis, Characterization, Structural, Electrochemical and Magnetic Studies of Monomeric $[Ni^{II}(1\text{-}MeIm)_6]Cl_2.H_2O$ Complex

A. S. Ganeshraja, K. Rajkumar, S. Thirumurugan, K. Anbalagan*

Department of Chemistry, Pondicherry University, Pondicherry, India

Received:03.05.2014 Accepted:05.08.2014

Abstract

Monomeric hexakis(1-methylimidazole)nickel(II) chloride monohydrate, $[Ni^{II}(1\text{-}MeIm)_6]Cl_2.H_2O$ has been synthesized and the geometry was determined using single crystal X-ray diffraction analysis. Spectral characterizations were made using FTIR, UV-vis, Raman analysis. Structure of the title complex consists; Ni atom is coordinated with six 1-methylimidazole ligands and two chloride ions are present in the outer sphere. Single-crystal X-ray diffraction refinement confirmed that the molecule belongs to monoclinic crystal system (crystal data: space group $P2_1/n$, $a = 8.0678(2)$ Å, $b = 13.2216(5)$ Å, $c = 15.0738(5)$ Å, $\alpha = \beta = 90°$, $\gamma = 97.816(3)°$, volume = 1592.98(9) Å, $z = 5$) with octahedral geometry. Strong photoluminescence (PL) was observed at 311 nm. Electrochemical reduction was measured using cyclic voltammeter. The complex shows magnetic hysteresis ($H_{ci} = 88.242$ Oe, $M_s = 4.62$ memu/g, $M_r = 4.84.87$ µemu/g) indicating the existence of ferromagnetism.

Keywords: *Monomeric nickel(II) octahedral complex; Crystal structure; Photoluminescence; Ferromagnetism.*

1. INTRODUCTION

Imidazole and its derivatives have played a formative role in the development of coordination chemistry and molecular biology (Steel *et al*. 1990; Kounavi *et al*. 2010). The variety of spectroscopic properties, stoichiometries and magnetic observed led to an improved understanding of the geometry, bonding and spin state in complexes and provided a touchstone for bonding theories, only few studies concerning the luminescence behavior of such complexes have been reported (Steel et al. 1990;). Imidazoles are particularly interesting ligands in bioinorganic and metallo supramolecular chemistry. Further, bioinorganic models may also lead to compounds which mimic enzyme function and provide new reagents or catalysts for practical application. In spite of the enormous scientific literature on metal complexes with simple imidazoles as ligands, there is in fact relatively little known about the coordination and metallosupramolecular chemistry of heavily substituted imidazoles (Steel *et al.* 1990). Generally Mn(II), Fe(III), Co(III), Ni(II), Cu(II) and Zn(II) imidazole complexes are important in areas such as biomedical, biological, and environmental applications (Buist *et al.* 2010). Occupational and/or environmental exposure to nickel has been implicated in various types of cancer (Giri *et al.* 2013). In vitro exposure to nickel compounds results in the accumulation of Ni(II) ions in cells, and recent studies have shown that Fe(II)- and αKG-dependent dioxygenases make up one group of major targets of Ni(II) ions inside the cell (Chen *et al*. 2009). Complexes of the type $Ni^{II}(imidazole)_6X_2$ (X = C1, Br, I, or NO_3) were readily obtained by precipitation with ether from ethanolic solutions. Attempts to prepare complexes containing a ligand-to-metal ratio of less than 6:1 were not successful by this method although pyridine readily forms complexes of the type $Ni(pyridine)_4X_2$ and $Ni(pyridine)_4X_2$. However, the complex $Ni^{II}(thiazole)_4Cl_2$ was obtained from a solution containing a 6 : 1 mole ratio. The present article reports the synthesis, characterization, photoluminescence, electrochemical and magnetic behavior of octahedral Ni(II)-1-methyl imidazoles complex.

* **K. Anbalagan** *Tel.: +914132654509*
E-mail: kanuniv@gmail.com

2. EXPERIMENTAL SECTION

2.1 Materials and methods

$NiCl_2.6H_2O$, 1-methyl imidazole (AR) and spectral grade KBr were purchased from Sigma Aldrich and used as received. Methanol and all other chemicals were purchased from Himedia and SD Fine Chemicals (India). Methanol was purified by repeated distillations over CaO. All other solvents were distilled before use and water was triply distilled over alkaline potassium permanganate in an all glass apparatus.

2.2 Instrumentation methods

Elemental analysis was performed on Thermo Scientific FLASH 2000 Organic Elemental Analyzer. The FTIR spectral investigations in the range 4000-400 cm^{-1} were made on a Thermo Nicollet-6700 FTIR instrument was obtained using KBr pellet technique (range 4000 to 400 cm^{-1}). Raman spectra were collected on the Jobin Yvon Horibra LABRAMR1100 micro-Raman spectrophotometer with laser source He-Ne 633 nm and argon 488 nm. Electronic absorption spectral studies were undertaken in a Shimadzu (model 2450) double beam spectrophotometer with quartz cells with integrating sphere attachment (Model ISR-2200) using complex concentration (~150 µM) in acetonitrile. Steady state fluorescence emission was recorded on Spex FluoroLog-3 spectrofluorometer (Jobin-Yvon Inc.) using 450 W xenon lamp and equipped with a Hamamatsu R928 photomultiplier tube. The instrument works on the principle of time-correlated single photon counting (TCSPC) technique. Time-resolved fluorescence decay measurement was carried out using Nano-LED (λ_{exc} = 295 nm) source for excitation (repetition rate 10 kHz). The photons were collected from the front face of the sample with TBX-4-X single-photon-counting detector. Life times were determined by fitting the data to exponential decay models using software packages. The goodness of fit was assessed by minimizing the reduced chi-squared function (χ^2) and visual inspection of the weighted residuals.

A crystal of $[Ni^{II}(1\text{-}MeIm)_6]Cl_2.H_2O$ complex with size 0.38 mm × 0.31 mm × 0.21 mm was mounted on an Oxford Diffraction Xcalibur diffractometer with an Eos (Nova) detector consists ω and φ scan mode in the range of $2.00° < \theta < 25.00°$. All diffraction measurements were performed at 293(2) K using graphite monochromated Mo-Kα radiation (λ = 0.71073 Å). A total of 7764 reflections were collected. The structure was solved by direct methods and refinement by full-matrix least squares on F^2 using 32-bit Olex2-1.1 version program. Hydrogen atoms were located from difference Fourier syntheses and included in the structure factor calculations with a riding model.

Cyclic voltammetry data were obtained using Autolab interface electrochemical analyzer consisting three electrode configuration such as; Pt working electrode (0.3 mm diameter), Pt electrode as auxiliary electrode and Ag/AgCl-KCl (sat.) reference electrode with Nova software, version: 2.9.3743-23, S. No. AUT84470. $[Ni^{II}(1\text{-}MeIm)_6]Cl_2.H_2O$ in DMSO, DMF and acetonitrile with 0.1 M tetra-(n-butyl)ammonium perchlorate (TBAP) background electrolyte was employed. The system was deoxygenated by purging with nitrogen gas for 10-15 min before measurement at sweep rates namely 50 to 350 mV s^{-1}. Magnetic measurements were carried out using vibrating sample magnetometer (Lakeshore-7404) in powder form; sample vibration frequency 82.5 Hz, dynamic range (1×10^{-7}) to 103 emu, maximum field at 1″ gap: 15 kOe in *dc* magnetic field. Magnetic susceptibilities on selected crystalline samples of $[Ni^{II}(1\text{-}MeIm)_6]Cl_2.H_2O$ in *dc* magnetic field were obtained under the selected field range ± 2000 Oe at the 298 K .

2.3 Preparation of $[Ni(1\text{-}MeIm)_6]Cl_2.H_2O$ complex

Dissolve 1 g of $NiCl_2.6H_2O$ in 3 ml. of EtOH. A little warming improves the rate of dissolution. Cool the solution in ice while adding 5 g (5.6 mL) of 1-methyl imidazole in EtOH. Additionally 1-methyl imidazole was slowly because the reaction is quite exothermic. After Cooling add 15 ml of cold ethanol to initiate crystallization. Keep cold for 10 min and collect the product on a Buchner funnel and wash with two 5 ml portions of ethanol. Finally Kept it in vaccum desiccators for a removal of moisture.

$[Ni(1\text{-}MeIm)_6]Cl_2.H_2O$; Recrystallized from ethanol to give green colored crystal, yield 0.84 g, 84%. *Calc. Anal.* for C_{24} H_{38} O_1 Ni N_{12} Cl_2: C 45.86, H 6.74, N 26.74, Cl 31.28 %. Found: C 45.05, H 6.53, N 25.32, Cl 32.98%. FTIR (KBr disc) cm^{-1}; 489.89(s), 565.77(s), 626.80(m), 676.28(m), 771.95(m), 818.14(w), 852.78(w), 936.90(m), 992.98(w), 1030.92(m), 1115.05(m), 1255.25(w), 1371.54(w), 1420.20(w), 1519.17(m), 1562.06(m), 1649.48(s), 1755.87(w), 1824.32(w), 1901.03(w), 2098.96(s), 2209.48(s), 2328.24(s), 2480.82(s), 2732.37(m), 3407(w), 3434.22(w), 3571.13(w). UV-vis (water medium: 0.001 M) λ_{max}, nm (ε_{max} $M^{-1}cm^{-1}$); free ligand 222.30 (9774), 269.41 (1697.01), complex (water medium: 0.001 M); 227.98 (3353), 270.47 (388), 277.34 (377), complex (water medium: 0.01 M);

304.42 (7.9), 380.42 (9.90), 632.74 (4.98). VSM data (298 K); χ_M = 0.76 cm^3 mol^{-1}, H_{ci} = 85.50 Oe, M_r = 1.61 × 10^{-3} emu, M_s = 3.56 × 10^{-3} emu.

3. RESULTS AND DISCUSSION

3.1 Spectral characterization

This sample was mulled in mineral oil or base, 1-methyl imidazole shows some vibration frequency in the ~1649 cm^{-1} region, one at 3434 cm^{-1} and another at 1519 cm^{-1}, both indicating coordinated amine groups and 2732 and 3571 cm^{-1} bands indicate lattice water. The FTIR spectrum of the complex shows characteristic absorption bands at 3407 and 566 cm^{-1}, assigned to ν (N-H) and ν (Ni-N) vibrations, respectively. This indicates that the atom coordinated with Ni(II) is the double bond nitrogen in the imidazole molecule. This is also conformed from single crystal X-ray analysis (Zhang *et al.* 2003). Whereas in the spectrum for the complex the –NH band occurs at 1562 cm^{-1}. This shift can be interpreted to be due to the imino groups. The sharp peaks found further indicate that all groups are alike and therefore coordinated. The shift of the ~3500 cm^{-1} peak to a lower frequency is indicative of an increase in electron localization of the –NH group upon coordination, as was noted by literature. Raman spectra of $[Ni^{II}(1\text{-}MeIm)_6]Cl_2$ is as shown in Figure 1. The peaks between 800 and 1600 cm^{-1} are due to enhanced ring stretches of the 1-methylimidazole as is evident by the lack of these features in the spectra of the 1-methylimidazole complex of $[Ni^{II}(1\text{-}MeIm)_6]^{2+}$. The intensities and frequencies of the imidazole peaks of both complexes more closely resemble the spectrum of free imidazole than that of imidazolium. Most of the bands of imidazole (Raman frequency of free ligand: 915, 1069, 1099, 1141, 1159, 1260, 1329, 1428, 1456, 1489, and 1530 cm^{-1}) (Jones *et al.* 1985). shift to slightly higher frequencies upon coordination (Raman frequency of $[Ni^{II}(1\text{-}MeIm)_6]Cl_2$: 920, 1068, 1098, 1121, 1142, 11621255, 1326, 1426, 1492, and 1537 cm^{-1}). The relative intensities of the vibrational bands are different for 1-methylimidazole and $[Ni^{II}(1\text{-}MeIm)_6]Cl_2$ complex (Walters *et al.* 1983). The *ca.* 1260 cm^{-1} mode is the most intense for free 1-methyl imidazole but is much weaker in the complex (Figure 1). For $[Ni^{II}(1\text{-}MeIm)_6]Cl_2$ complex relative intensities of the ring modes change with excitation wavelength.

The electronic absorption spectrum of $[Ni(1\text{-}MeIm)_6]^{2+}$ is given in Figure 2. Which shows free ligand bands at 222 nm with high absorption coefficient value and at 269 nm with low absorption coefficient value in neat water (0.001 M), complex has bands at λ_{max} at 228, 270 and 304 nm with high absorption coefficient value due to $\pi \rightarrow \pi^*$ and

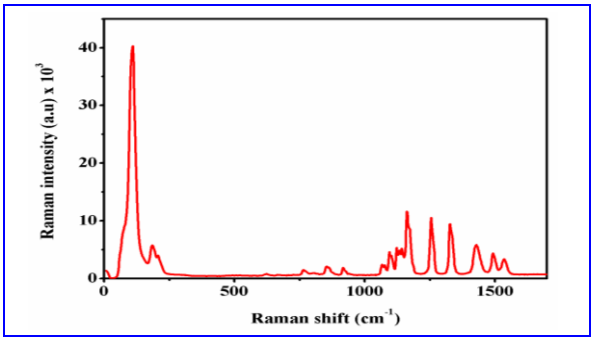

Fig. 1: Raman spectrums of $[Ni(1\text{-}Meim)_6]Cl_2.H_2O$ complex.

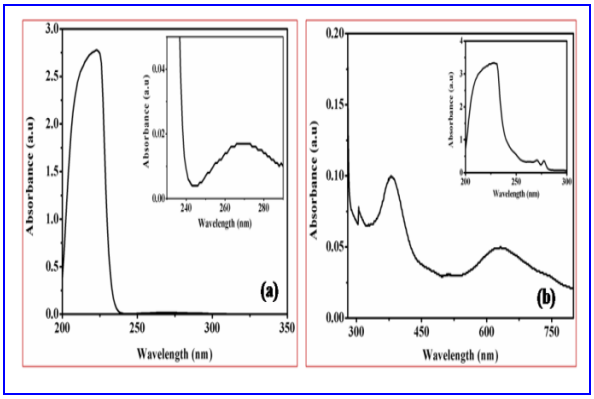

Fig. 2: UV-visible spectra of (a) free ligand of 1-methyl imidazole (0.001 M) and (b) $[Ni(1\text{-}Meim)_6]Cl_2.H_2O$ complex (0.001 and 0.01 M) in neat water at 298 K.

LMCT transitions of $[Ni(1\text{-}MeIm)_6]^{2+}$ in neat water at lower concentration. The lower energy level d-d transitions of $[Ni(1\text{-}MeIm)_6]^{2+}$ observed at 380 and 633 nm in neat water (0.01 M). This is indicate that Ni(II)-1-methyl imidazole complex have octahedral geometry.

The photoluminescence behavior of the free ligand (1-MeIm) (Figure 3(a)) and its corresponding nickel(II) complex ion of $[Ni^{II}(1\text{-}MeIm)_6]^{2+}$ in neat water (1 mM) solution at room temperature is depicted in Figure 3(b). The compound exhibit intense luminescence. Upon photo excitation at the corresponding absorption band (268 nm), the free ligand exhibits a very weak fluorescent emission, whereas compound show more intense photoluminescence with main emissions at 312 nm (λ_{exc} = 276 nm) and 430, 543, 625 nm (λ_{exc} = 380 nm) as presented in Table 1, Figure 3(c). The complex shows *d-d* absorption features at ~380 nm can be

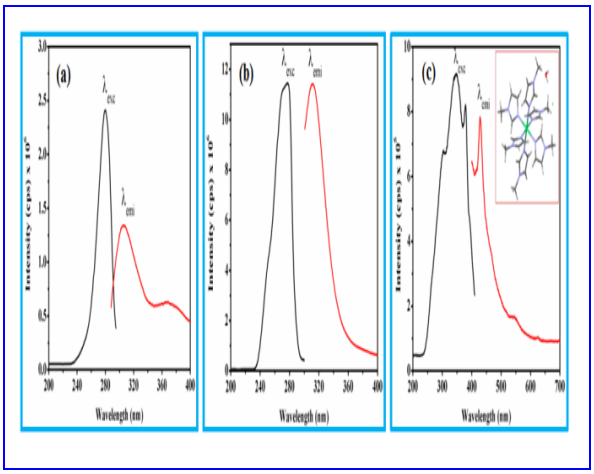

Fig. 3: ***Emission spectrum of (a) free ligand of 1-methyl imidazol excitation at 268 nm, (b) Ni(1-Meim)$_6^{2+}$ complex excitation at 270 nm and (c) at 380 nm in water (0.001 M) at 298 K.***

Table 1. ***Emission spectral data of free ligand and [Ni(1-MeIm)$_6$]$^{2+}$ in water (0.001 M).***

Compound	λ_{exc} nm	λ_{emi} nm	Intensity (cps) × 10^5
1-methyl imidazole (λ_{exc} = 268 nm)	279.58	306.02	13.48
complex (λ_{exc} = 270 nm)	276	311.52	114.40
complex (λ_{exc} = 380 nm)	302.97 347.42 379.26	429.09 543.41 624.97	7.83 1.71 1.07

assigned to the spin allowed transition state, and also exhibiting three emissions at 429, 543 and 625 nm. The 429 nm emission with lifetime in the microsecond region is attributable to phosphorescence, while the shorter wavelength band at 380 nm with lifetime <10 ns is assigned to fluorescence from the singlet excited state (Xia *et al*. 2002, Powers *et al*. 2013).

3.2 X-ray crystal structure of the title complex

The X-ray structure of the complex [Ni(1-MeIm)$_6$]Cl$_2$ is built up of discrete monomeric molecules. Figure 4(a) shows a perspective view of the title compound with atomic numbering scheme and Figure 4(b) a perspective view of the crystal packing in the unit cell. The space group, unit cell are

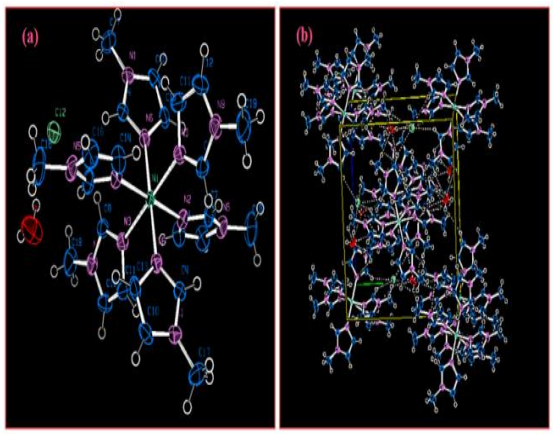

Fig. 4: (a) Ortep and (b) packing diagram of of [Ni(1-Meim)$_6$]Cl$_2$.H$_2$O complex.

presented in Tables 2. The crystal structure of the complex consists of [Ni(1-MeIm)$_6$]$^{2+}$ cation and two chloride anions, linked by electrostatic forces and hydrogen bonds (shown as dashed lines in Figure 4(a)). The coordination model of the nickel(II) can be described as being of octahedral geometry. Six 1-methylimidazole molecules are coordinated through their tertiary nitrogen atoms to each nickel(II) ion, and two chloride anions are out of the coordination sphere and balance the charge. One water molecule is present in lattice and stabiles crystal through hydrogen interaction with complex molecular cation. The bond distances of Ni(1)-N(2), Ni(1)-N(2^1), Ni(1)-N(3) = Ni(1)-N(3^1), Ni(1)-N(6) = Ni(1)-N(6^1). of [Ni(1-MeIm)$_6$]Cl$_2$ are 2.1346(17), 2.1346(17), 2.1612(18) and 2.1240(17) Å, respectively. These distances are in agreement with those reported for octahedral [Ni(Im)$_6$]$^{2+}$ complex [2.120(1), 2.124(1), 2.141(1) Å] for [Ni(Im)$_6$](sal)$_2$ (sal = salicylate) (Jian *et al.* 1999) and 2.133(3), 2.132(3) and 2.125(3) Å for [Ni(Im)$_6$](dtp)$_2$ (dtp = O,O′-diphenyldithiophosphate) (Zhang *et al.* 2003).

Table 2. ***Crystal data and structure refinement for [Ni(1-MeIm)$_6$]Cl$_2$.H$_2$O.***

Empirical formula	$C_{12}H_8N_2Cl_2CoO_{0.2}Ni_{0.2}$
Formula weight	324.98
Temperature / K	293(2)
Crystal system	monoclinic
Space group	$P2_1/n$
a / Å, b / Å, c / Å	8.0678(2), 13.2216(5), 15.0738(5)
α/°, β/°, γ/°	90.00, 97.816(3), 90.00
Volume / Å^3	1592.98(9)
Z	5
ρ_{calc} / mg mm^{-3}	1.694
μ / mm^{-1}	2.030
F(000)	811
Crystal size / mm	0.38 × 0.31 × 0.21
2Θ range for data collection	5.96 to 50°
Index ranges	-9 ≤ h ≤ 9, -15 ≤ k ≤ 13, -17 ≤ l ≤ 16
Reflections collected	7163
Independent reflections	2802 [R(int) = 0.0257]
Data/restraints/parameters	2802/0/198
Goodness-of-fit on F^2	1.081
Final R indexes [I>2σ (I)]	R_1 = 0.0381, wR_2 = 0.0972
Final R indexes [all data]	R_1 = 0.0440, wR_2 = 0.1015

3.3 Electrochemical and magnetic analysis

Electron transfer process of the nickel(II) complex was determined in acetonitrile, DMSO and DMF solutions using cyclic voltammetry at a platinum working electrode under inert atmosphere. The electrochemical data are presented in Tables 3-5 and the voltammetric behavior of a representative complex $[Ni^{II}(1\text{-MeIm})_6]^{2+}$ is shown in Figure 5. Figure 5 show the cyclic voltammograms recorded for the $[Ni^{II}(1\text{-MeIm})_6]^{2+}$ complex ion at the sweep rate of 50 to 350 mV s^{-1} in acetonitrile, DMSO and DMF solution. Owing to the redox-active nature of the 1-methylimidazole, ligand-based electrochemical activity is expected in the complex (Ganeshraja *et al*. 2013, Anbalagan *et al*. 2013). Cyclic voltammetry experiments show that the $[Ni^{II}(1\text{-MeIm})_6]^{2+}$ complex is electrochemically active and can be reduced at potentials of at –1056 to -1211, -857 to -1107, -605 to -666 mV in acetonitrile, DMSO and DMF respectively. In DMF the cyclic voltammogram of the $[Ni^{II}(1\text{-MeIm})_6]^{2+}$, shows reversible oxidation and reduction processes for the $Ni^{II/I}$ couple allowing the determination of the half-wave potential as $E_{1/2}$ = -1007 to -1142 mV in acetonitrile (with respect to reference electrode). The nature and reduction potential of $[Ni^{II}(1\text{-MeIm})_6]^{2+}$ is similar to that observed for mononuclear nickel(II) complexes and attributable to the Ni^{II}/Ni^{I} redox couple (Gennari *et al.* 2010, Jenkins *et al*. 2009). In the present case the ΔE_p values for this couple are also very large (Tables 3-5). In some cases during cyclic voltammetric reduction of nickel(II) complex, the reoxidative anodic wave is observed but with large peak-to-peak separations (ΔE) (Simon-Manso *et al*. 2005, Gomez *et al*. 1997). The detailed study of the electrochemical properties of nickel(II)-1-MeIm complex indicated that the complex is electrochemically active in acetonitrile, DMSO and DMF.

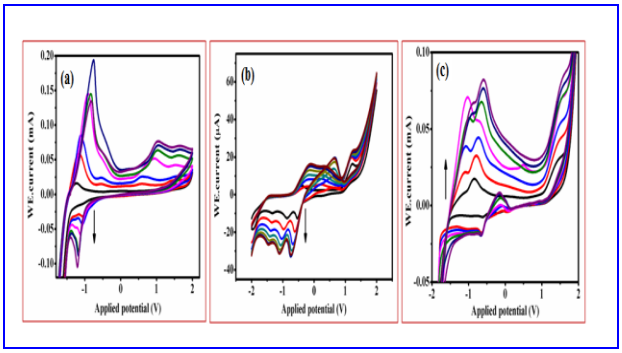

Fig. 5: Cyclic voltammograms of Ni(1-Meim)$_6^{2+}$; sweep rates 50 to 350 mV s^{-1}. Pt working electrodes in (a) acetonitrile, (b) DMSO and (c) DMF (1 mM) solvents and supporting electrolyte 0.1 M tetra-(n-butyl) ammonium perchlorate.

The variation of induced magnetic moment with respect to the applied magnetic field would be identified by vibrating sample magnetometer for the analysis of magnetic nature of the material (Anbalagan *et al*. 2010).

The observed magnetization nature of the $[Ni^{II}(1\text{-MeIm})_6]^{2+}$ complex is shown in Figure 6. The complex is found to be ferromagnetic with molar magnetic susceptibility χM = 0.76 cm^3 mol^{-1}, coercivity Hci = 85.50 Oe and saturation magnetization 3.56 memu at 298 K. It is observed that the intensity of magnetization varies nonlinearly with the applied field, which shows the ferromagnetic

Table 3. Electrochemical data for the [Ni(1-MeIm)$_6$]Cl$_2$ complex in acetonitrile

scan rate, mV s^{-1}	E_{pa}, mV	E_{pc}, mV	ΔE_p, mV	E_f, mV
50	1369	1176	193	1273
	-1227	-1056	-171	-1142
100	596	465	131	531
	-1167	-1067	-1	-1117
150	651	386	265	519
	-1108	-1068	-04	-1088
200	936	653	283	795
	-917	-1127	-21	-1022
250	1016	675	341	846
	-837	-1176	-339	-1007
300	1056	642	414	849
	-756	-1188	-432	-972
350	1016	622	394	819
	-826	-1211	-385	-1019

Table 4. *Electrochemical data for the Ni(1-MeIm)$_6^{2+}$ in DMSO*

scan rate, mV s^{-1}	E_{pa}, mV	E_{pc}, mV	ΔE_p, mV	E_f, mV
50	1227	-395	1662	416
	906	-536	1442	185
	-	-857	-	-429
	-	-1327	-	-664
100	1207	886	321	161
	225	-617	842	-196
	-245	-977	-732	-611
	-1427	-1347	-80	-1387
150	1216	927	289	1072
	224	-686	910	-231
	-178	-1026	-848	-602
	-1447	-1387	-60	-1417
200	1227	956	271	1092
	296	-716	-420	-210
	-145	-1067	-922	-606
	-1438	-1417	-60	-1418
250	1237	966	271	1102
	296	-737	-441	-221
	-135	-1097	-962	-616
	-1407	-1437	-30	-1422
300	1246	966	280	1106
	356	-737	1093	-191
	-155	-1097	-942	-626
	-1417	-1428	-11	-1423
350	1246	966	280	1106
	335	-746	1081	-206
	-125	-1107	-982	-616
	-1427	-1458	-31	-1443

Table 5. *Electrochemical data for the [Ni(1-MeIm)$_6$]Cl$_2$ complex in DMF.*

scan rate, mV s^{-1}	E_{pa}, mV	E_{pc}, mV	ΔE_p, mV	E_f, mV
50	1.486	1.096	390	1291
	-836	-605	-231	721
100	1515	1086	429	1301
	-786	-646	-140	716
150	1527	1107	420	1317
	-726	-647	-79	687
200	1542	1077	465	1310
	-1032	-646	-386	841
250	1587	1107	480	1347
	-656	-647	-9	652
300	1607	1147	460	1377
	-596	-656	-60	626
350	1597	1156	441	1377
	-605	-666	-61	636

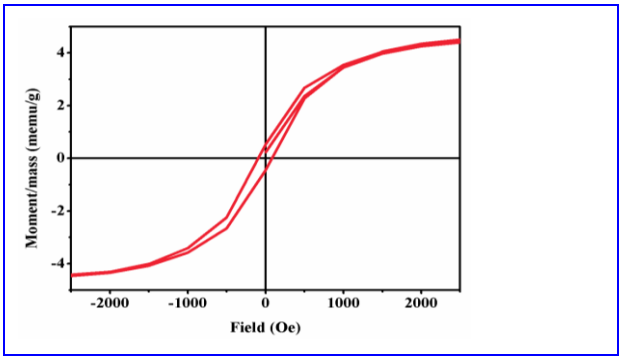

Fig. 6: Hysteresis loop for the compound [Ni(1-Meim)$_6$]Cl$_2$.H$_2$O in dc magnetic field.

nature at room temperature. Mononuclear nickel(II) complex with 1-metylimidazole ligand consist discrete $Ni^{II}N_6^{2+}$ units show ferromagnetic nature. Figure 6 illustrates in the hysteresis loop of $[Ni^{II}(1\text{-MeIm})_6]^{2+}$ complex, although response is weak, is distinct evidence of the weak ferromagnetic ordering at room temperature (298 K) (Dockum *et al*. 1982).

4. CONCLUSION

Dipositive nickel combines with 1-methylimidazole ligand and yields stable, crystalline solid with octahedral geometry. Complexation of the imidazole moiety with Ni(II) was identified using FTIR, electronic absorption spectra and

photoluminescence spectra at 298 K. Electronic spectral measurement in neat water of the $[Ni^{II}(1\text{-}MeIm)_6]^{2+}$ complex illustrates d-d transitions with low ϵ values. The structure of the complex has been established by single-crystal X-ray diffraction refinement and confirmed to be triclinic crystal form with octahedral geometry. $[Ni^{II}(1\text{-}MeIm)_6]^{2+}$ complex was synthesized using modified methods, which were found to show interesting luminescent features and ferromagnetism in conjunction with magneto-structural chracteristics. Electrochemical analysis of the nickel(II) complex illustrated that the complex (ΔEp increases) becomes highly irreversible in reduction process. The current functions are independent of sweep rate (50-350 mV s^{-1}) which is an indication of a simple one electron transfer. This investigation establishes that emission, electrochemical reduction and magnetic properties of $[Ni^{II}(1\text{-}MeIm)_6]^{2+}$ complex.

ACKNOWLEDGEMENT

K. Anbalagan is thankful to the Council of Scientific and Industrial Research (No. 01(2570)/12/EMR-II dt. 03.04.2012) New Delhi for financial support through major research project. The authors thank DST-FIST, Department of Chemistry and CIF, Pondicherry University for providing instrumental facility.

REFERENCE

Steel, P. J., Aromatic nitrogen heterocycles as bridging ligands; a survey, Coord. Chem. Rev., 106, 227–265 (1990). doi:10.1016/0010-8545(60)80005-7

Buist, D., Williams, N. J., Reibenspies, J. H. and Hancock, R. D., Control of Metal Ion Size-Based Selectivity through Chelate Ring Geometry. Metal Ion Complexing Properties of 2,2′-Biimidazole, Inorg. Chem., 49, 5033–5039 (2010). doi:10.1021/ic100131z

Giri, N. C., Passantino, L., Sun, H., Zoroddu, M. A., Costa, M. and Maroney, M. J., Structural Investigations of the Nickel-Induced Inhibition of Truncated Constructs of the JMJD2 Family of Histone Demethylases Using X-ray Absorption Spectroscopy, Biochemistry, 52, 4168−4183 (2013). doi:10.1021/bi400274v

Chen, H. and Costa, M., Iron and 2-Oxogluterate Dependent Dioxygenases: An Emerging Group of Molecular Targets of Nickel Toxicity and Carcinogenicity, Proceedings of Biometals, 22, 191−196 (2009). doi:10.1007/s10534-008-9190-3

Zhang, S., Wang, S., Wen, Y. and Jiao, K., Synthesis and Crystal Structure of Hexakis(imidazole) nickel(II) O,O′-diphenyldithiophosphate [Ni(Im)6](Ph2O2PS2)2, Molecules, 8, 866-872 (2003). doi:10.3390/81200866

Jones, C. M., Johnson, C. R., Asher, S. A. and Shepherd, R. E., Resonance Raman Studies of the Excited Electronic States of (CN),FeIII(imidazole)2- and (NH3)5RuIII(imidazole)3+, J. Am. Chem. Soc. 107, 3772-3780 (1985). doi:10.1021/ja00299a005

13) M. A. Walters and T. G. Spiro, 1983. "Resonance Raman enhancement of imidazole vibrations via charge-transfer transitions of pentacyanoiron(III) imidazole and imidazolate complexes", Inorg. Chem., 22: 4014-4017. doi:10.1021/ic00168a039

Xia, B. H., Che, C. M., Phillips, D. L., Leung, K. H. and Cheung, Metal−Metal Interactions in Dinuclear d8 Metal Cyanide Complexes Supported by Phosphine Ligands. Spectroscopic Properties and ab Initio Calculations of [M2(μ-diphosphine)2(CN)4] and trans-[M(phosphine)2(CN)2] (M = Pt, Ni), Inorg. Chem., 41, 3866-3875 (2002). doi:10.1021/ic020077j

Powers, D. C., Anderson, B. L. and Nocera, D. G., Two-Electron HCl to H2 Photocycle Promoted by Ni(II) Polypyridyl Halide Complexes, J. Am. Chem. Soc., 135, 18876−18883 (2013). doi:10.1021/ja408787k

Jian, F. F., Wang, Z. X., Bai, Z. P. and You, X. Z., Structure of hexakis(imidazole)nickel(II) disalicylate, [Ni(Im)6](Sal)2, J. Chem. Cryst., 29, 359-365 (1999). doi:10.1023/A:1009542422416

Anbalagan, K., Ganeshraja, A. S., Electron-rich ligand modified, ferromagnetic luminescent cis-[CoIII(en)2(RNH2)Cl]Cl2 complexes and their electrochemical reduction behavior, Inorg. Chem. Commu. 37, 59-65 (2013). doi:10.1016/j.inoche.2013.09.029

Gennari, M., Orio, M., Pecaut, J., Neese, F., Collomb, M. N., and Duboc, C., Reversible Apical Coordination of Imidazole between the Ni(III) and Ni(II) Oxidation States of a Dithiolate Complex: A Process Related to the Ni Superoxide Dismutase, Inorg. Chem., 49, 6399–6401 (2010). doi:10.1021/ic100945n

Jenkins, R. M., Singleton, M. L., Almaraz, E., Reibenspies, V., and Darensbourg, M. Y., Imidazole-Containing (N3S)-NiII Complexes Relating to Nickel Containing Biomolecules, Inorg. Chem., 48, 7280–7293 (2009). doi:10.1021/ic900778k

Simon-Manso, E. and Kubiak, C. P., Dinuclear Nickel Complexes as Catalysts for Electrochemical Reduction of Carbon Dioxide, Organometallics, 24, 96-102 (2005). doi:10.1021/om0494723

Gomez, M., Muller, G., Panyella, D., and Rocamora, M., New Open Tetraaza Nickel(II) and Palladium(II) Complexes. Different Reactivity of the Electrogenerated M(0) Species toward Difunctional Substrates", Organometallics, 16, 5900-5908 (1997). doi:10.1021/om9707026

Anbalagan, K., UV-Sensitized Generation of Phasepure Cobalt-Doped Anatase: CoxTi1-xO2-δ Nanocrystals with Ferromagnetic Behavior Using Nano-TiO2/cis-[CoIII(en)2(MeNH2)Cl]Cl2", J. Phys. Chem., 115, 3821-3832 (2011). doi:10.1021/jp1064227

Dockum, B. W. and Reiff, W. M., Thiocyanate-bridged transition-metal polymers. 3. Structure and low-temperature magnetic properties of Ni(bpy)(NCS)2: an infinte-chain ferromagnetic insulator, Inorg. Chem., 21, 2613-2619 (1982). doi:10.1021/ic00137a017